Orthorhombic elastic constants of an NbTi/Cu composite superconductor

H. M. Ledbetter and D. T. Read*

Cryogenics Division, Institute for Basic Standards, National Bureau of Standards, Boulder, Colorado 80302
(Received 18 October 1976; accepted for publication 11 January 1977)

Elastic properties of a niobium-titanium-filament copper-matrix composite superconductor were studied experimentally at room temperature. Ultrasonic pulse and resonance measurements showed the material has orthorhombic symmetry and, therefore, nine independent elastic constants. With respect to copper, C_{11}, C_{22}, and C_{33} are about 7% lower; C_{44}, C_{55}, and C_{66} are about 15% lower; the off-diagonal elastic constants are the same; and the bulk modulus is about 5% lower. Deviations from isotropic elastic behavior are small.

PACS numbers: 62.20.Dc, 74.70.Rv, 74.30.Gn

I. INTRODUCTION

The purpose of this paper is to report a room-temperature experimental study of the elastic properties of a composite material. The study emphasizes elastic symmetry and applies familiar single-crystal methods to composites. The studied composite has unidirectional niobium-titanium (NbTi) filaments in a copper (Cu) matrix and it is designed as a superconductor for magnets. Manufacture and morphology suggest that the filament direction is an elastic-symmetry axis. Thus, the macroscopic elastic symmetry is orthorhombic, tetragonal, hexagonal, or cubic. Oblique axis systems—triclinic, monoclinic, trigonal—are excluded.

The present study shows that the studied composite is orthorhombic, but deviations from isotropy are small, and it can be referred to other coordinate axes (for example, hexagonal) without introducing large errors; advantages of this simplification are discussed in Sec. V Nevertheless, a complete set of nine orthorhombic elastic constants was determined. The elastic constants reported here may differ from those of apparently identical composites for reasons discussed in Secs. III C and V F.

Experimentally, two dynamic methods were used: pulse and resonance. Most measurements were made by a pulse method; 18 ultrasonic wave velocities were measured along the orthorhombic ⟨100⟩ and ⟨110⟩ directions. Resonance experiments were done for two reasons: to look for dispersion, the variation of sound-velocity with frequency, and to confirm the off-diagonal elastic constants.

II. WAVE MOTION IN ORTHORHOMBIC MEDIA

Usual crystallographic notations for vectors and elastic constants are used in this paper. Since all components of the studied composite are polycrystalline, the symmetries discussed here are strictly macroscopic. The filament direction of the composite is designated [001], and the principal directions perpendicular to the filaments are [100] and [010]. These directions are indicated in Fig. 1.

As stated above, the studied material has orthorhombic symmetry, and, therefore, nine independent elastic constants. These are displayed in Eq. (1) in the Voigt contracted notation in matrix form.

$$C_{ij}=\begin{bmatrix} C_{11} & C_{12} & C_{13} & 0 & 0 & 0 \\ & C_{22} & C_{23} & 0 & 0 & 0 \\ & & C_{33} & 0 & 0 & 0 \\ & & & C_{44} & 0 & 0 \\ & & & & C_{55} & 0 \\ & & & & & C_{66} \end{bmatrix}, \tag{1}$$

where the matrix is symmetrical about its main diagonal. The Christoffel equations, which relate the elastic constants to the plane monochromatic phase velocities, are[1]

$$(C_{ijkl}n_jn_k-\rho v^2\delta_{il})p_l=0, \tag{2}$$

where C_{ijkl} is the fourth-rank elastic-stiffness tensor, n is the wave-propagation direction, ρ is the mass density, v is the wave velocity, δ_{il} is the Kronecker delta,

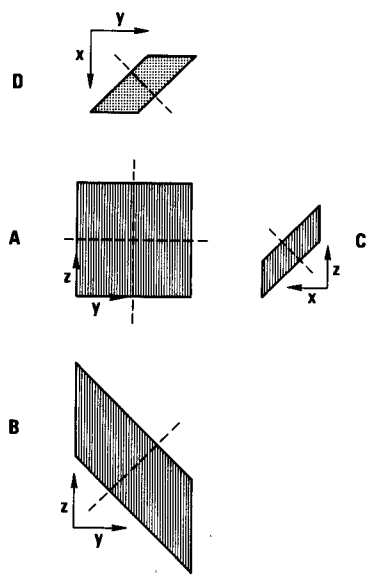

FIG. 1. Schematic geometries of four pulse specimens. Filaments along [001] are indicated by striping. The wave-propagation directions (indicated by dashed lines) and displacement vectors are given in Table I. The x, y, and z axes are equivalent to the [100], [010], and [001] axes that are used in the text and tables.

and p is the displacement vector. It is easy to show that the resulting secular equation is diagonal for the [100], [010], and [001] directions; that is, waves traveling along ⟨100⟩ directions are pure modes. Their velocities are determined by C_{11}, C_{55}, C_{66}; C_{22}, C_{44}, C_{66}; and C_{33}, C_{44}, C_{55}, respectively. Thus, all diagonal elastic constants, C_{ii}, can be determined by propagating waves in ⟨100⟩ directions. For each direction there is one longitudinal wave and there are two shear waves; the three waves are polarized mutually orthogonally. Thus, checks on each of the three shear elastic constants, C_{44}, C_{55}, and C_{66}, are available. The off-diagonal elastic constants C_{12}, C_{13}, and C_{23} must be determined by measurements where the n vectors are oblique to ⟨100⟩ directions.

In general, waves traveling along lower-symmetry directions are not pure modes.[2] For $\mathbf{n}=\langle 110\rangle$, there is a single pure mode whose velocity is determined by $\frac{1}{2}(C_{55}+C_{66})$, $\frac{1}{2}(C_{44}+C_{66})$, and $\frac{1}{2}(C_{44}+C_{55})$ for the [011], [101], and [110] directions, respectively. These provide additional checks on the three C_{ii} shear constants measured along ⟨100⟩ directions. The two impure modes that propagate along each ⟨110⟩ direction can be determined from the Christoffel equations.

The ⟨011⟩ propagation-direction case is now outlined. The Kelvin-Christoffel elastic stiffnesses

$$\Gamma_{il}=C_{ijkl}n_j n_k \tag{3}$$

are for the case $\mathbf{n}=(1/\sqrt{2})\,[011]$:

$$\Gamma_{il}=\tfrac{1}{2}\begin{bmatrix} C_{55}+C_{66} & 0 & 0 \\ 0 & C_{22}+C_{44} & C_{23}+C_{44} \\ 0 & C_{23}+C_{44} & C_{33}+C_{44} \end{bmatrix}. \tag{4}$$

Thus, one solution is

$$\rho v^2=\tfrac{1}{2}(C_{55}+C_{66}), \tag{5}$$

a torsion mode. And the remaining two roots are

$$\rho v^2=\tfrac{1}{2}\{C_{22}+C_{33}\pm[(C_{22}-C_{33})^2 +4(C_{23}+C_{44})^2]^{1/2}\}+C_{44}. \tag{6}$$

Experimentally, ρv^2 is measured and C_{23} is unknown. Thus, by rearrangement,

$$C_{23}=\pm\{[2\rho v^2-\tfrac{1}{2}(C_{22}+C_{33}+2C_{44})]^2 -\tfrac{1}{4}(C_{33}-C_{22})^2\}^{1/2}-C_{44}. \tag{7}$$

The spurious second value of C_{23} from this equation can be discarded on physical grounds. Similarly, [101] and [110] planes can be used to determine C_{13} and C_{12}, respectively. For these cases

$$C_{13}=\pm\{[2\rho v^2-\tfrac{1}{2}(C_{11}+C_{33}+2C_{55})]^2 -\tfrac{1}{4}(C_{33}-C_{11})^2\}^{1/2}-C_{55} \tag{8}$$

and

$$C_{12}=\pm\{[2\rho v^2-\tfrac{1}{2}(C_{11}+C_{33}+2C_{66})]^2 -\tfrac{1}{4}(C_{22}-C_{11})^2\}^{1/2}-C_{66}. \tag{9}$$

Further details on the problem of wave propagation in orthorhombic media were given by Musgrave.[3]

III. EXPERIMENTAL

A. Material

The samples used in this study were cut from a short section of a Kryo 210 superconductor. (A trade name is used to describe the studied material; its use is not an NBS endorsement of the product.) This is a copper-matrix niobium-titanium-filament composite material. The Cu/NbTi volume ratio is 6:1, and the bar contains 2640 filaments with a twist each 7.6 cm. The filament distribution is shown in Fig. 2. The sample obtained for this study was about 20 cm long, 1.0 cm wide, and 0.5 thick. Four samples were cut for ultrasonic pulse measurements, one with its surfaces perpendicular to the symmetry axes of the material and three with the largest surface oriented at 45° to two symmetry axes. Sample geometries are shown in Fig. 1. Samples were studied in the as-received condition, that is, optimized by the manufacturer for use as a superconductor. The thermal and mechanical treatments that optimize such superconductors were described by McInturff and Chase.[4] The specimen with {100} surfaces was 0.5 ×1.0×1.0 cm, while the three off-axis specimens had thicknesses of 5, 3, and 2 mm. All specimens were ground sufficiently flat and parallel for ultrasonic study.

B. Procedures

Eighteen ultrasonic-wave modes were studied in these four specimens at room temperature. Quartz-crystal transducers either 9.5 or 6.4 mm in diameter with fundamental resonance frequencies between 5 and 10 MHz were bonded to one specimen surface with phenyl salicylate (salol). Ultrasonic pulses were generated and detected in the transducer using an electronic apparatus described previously.[5] The time interval between the arrival of selected pulses from the ultrasonic echo train was measured using an oscilloscope with a delaying time base calibrated against a precision time-mark

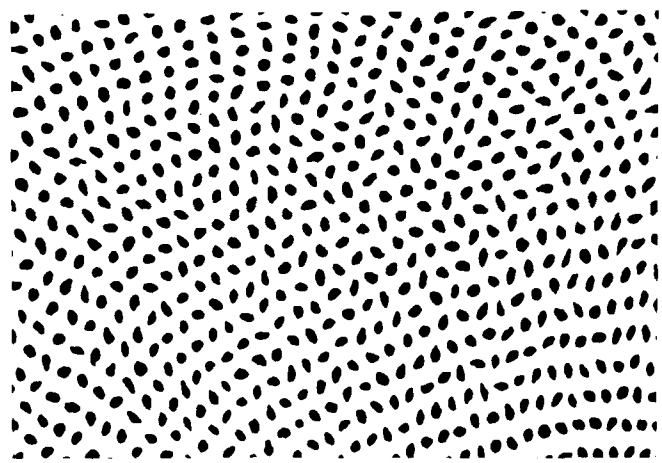

FIG. 2. Photomicrograph showing distribution of filaments. Plane of photo is perpendicular to filaments. Width shown corresponds to 4.3 mm in specimen. Vertical direction is $x=[100]$ and horizontal direction is $y=[010]$.

TABLE I. Room-temperature elastic constants C_{ij} for a NbTi/Cu composite with macroscopic orthorhombic symmetry. The wave-front normal is denoted by **n** and the displacement direction by **p**. Both ρv^2 and C_{ij} have units of 10^{11} N/m^2.

Specimen	Measurement number	n	p	ρv_l^2	ρv_t^2	C_{ij}	Derived C_{ij}
A	1	100	100	1.834		C_{11}	$C_{11} = 1.834 \pm 0.005$
	2		010		0.404	C_{66}	$C_{66} = 0.414 \pm 0.007$
	3		001		0.407	C_{55}	$C_{55} = 0.407 \pm 0.011$
	4	010	010	1.878		C_{22}	$C_{22} = 1.878 \pm 0.015$
	5		100		0.413	C_{66}	
	6		001		0.413	C_{44}	$C_{44} = 0.416 \pm 0.003$
	7	001	001	1.880		C_{33}	$C_{33} = 1.880 \pm 0.002$
	8		100		0.414	C_{55}	
	9		010		0.419	C_{44}	
B	10	011	011[a]	1.713		$\frac{1}{2}\{C_{22}+C_{33} \pm [(C_{22}-C_{33})^2+4(C_{23}+C_{44})^2]^{1/2}\}+C_{44}$	$(C_{23} = 0.715)$[b]
	11		$0\bar{1}1$[a]		0.419		$C_{23} = 1.041 \pm 0.040$
	12		100		0.407	$\frac{1}{2}(C_{55}+C_{66})$	
C	13	101	101[a]	1.740		$\frac{1}{2}\{C_{11}+C_{33} \pm [(C_{11}-C_{33})^2+4(C_{13}+C_{55})^2]^{1/2}\}+C_{55}$	$(C_{13} = 0.809)$[b]
	14		$\bar{1}01$[a]		0.409		$C_{13} = 1.039 \pm 0.040$
	15		010		0.408	$\frac{1}{2}(C_{44}+C_{66})$	
D	16	110	110[a]	1.744		$\frac{1}{2}\{C_{11}+C_{22} \pm [(C_{11}-C_{22})^2+4(C_{12}+C_{66})^2]^{1/2}\}+C_{66}$	$(C_{12} = 0.804)$[b]
	17		$1\bar{1}0$[a]		0.400		$C_{12} = 1.056 \pm 0.040$
	18		001		0.394	$\frac{1}{2}(C_{44}+C_{55})$	

[a] Impure modes.

[b] Values discarded for reasons discussed in text.

generator. The ultrasonic echo patterns obtained in this study were of good quality. They had between 3 and 30 well-defined echoes.

Using the velocity v of the ultrasonic wave (obtained from the transit time and the path length) and the specimen mass density ρ, the room-temperature elastic constants were calculated from

$$C = \rho v^2, \tag{10}$$

a simplified form of Eq. (2), where C is a combination of the C_{ij}'s depending on the mode. Results derived from Eq. (2) for the 18 modes studied here are given in Table I.

Resonant-bar elastic-constant measurements were performed on two other specimens at room temperature. These specimens were 4.8-mm-diam cylinders with lengths of 1.9 and 3.1 cm prepared with filaments along the specimen axis. In the resonant-bar technique, the sample is excited into longitudinal or torsional resonance by an attached quartz-crystal driver of appropriate mode and frequency. Resonance is detected using a quartz gauge crystal attached to the driver. The driver, gauge, and specimen form a composite oscillator. The appropriate elastic constant of the specimen can be calculated from the resonant frequency of the composite oscillator, the specimen density, and known properties of the driver and gauge crystals. Since the composite-oscillator resonant frequency is often tens of kilohertz, this technique is sometimes called a kilohertz technique, but it is called a composite-oscillator technique in the literature.[6] No correction was made for specimen geometry. According to the well-known formulas of Rayleigh, in this case, the correction multiplier is 1.003 for Young's moduli and 1.000 for torsional moduli.

C. Uncertainties

Experimental uncertainties of the elastic constants are discussed in two parts: imprecision and systematic error. Imprecisions affect many conclusions of the study; systematic errors do not; they affect only the C_{ij}'s themselves.

Bounds on the C_{ij}'s in Table I are imprecisions expressed as $\pm\sigma$, where σ is the standard deviation based on a normal distribution. For the diagonal C_{ij}'s, these imprecisions are based on two to five pure-mode measurements. Imprecisions of the nondiagonal C_{ij}'s depend both on these values and on an assumed imprecision of 0.005 in the quasitransverse values of ρv^2. Sources of imprecision include deviations of specimens from flat and parallel, specimen-length mismeasurements, specimen-to-specimen bond variations, transit-time mismeasurement, and, for this material, specimen inhomogeneity.

There are two principal systematic errors, one arising from the mass density and one from the transducer-bond coupling to the specimen. Maximum error in the mass density is estimated to be less than 0.15%. Transit-time error due to the ultrasonic wave traveling through the transducer and the coupling agent is estimated to be less than 1%; and, when corrected for, increases the ρv^2 values. Thus, the overall uncertainty in the C_{ij}'s is estimated to be less than $\pm 1.5\%$.

A possible source of sample-to-sample variation in the elastic constants of any composite material is its thermal-mechanical treatment, which may vary considerably for the type of material reported on here. For example, for copper, elastic-constant differences up to 10% have been reported for annealed and deformed specimens.[7] Such variations can also occur in copper-base composites. Residual stresses of the order of the yield strength may occur in the composite, but simple

TABLE II. Elastic compliances of a NbTi/Cu composite measured by a resonance method at room temperature. Units are 10^{-11} m^2/N.

S_{ij}	Observed	Calculated from C_{ij}'s
S_{33}	0.873 ± 0.009	0.878 ± 0.073 from quasishear modes (0.692 from quasilongitudinal modes)
$\frac{1}{2}(S_{44}+S_{55})$	2.398 ± 0.024	2.430 ± 0.041

computations show that these would change the elastic constants by less than 1%.

IV. RESULTS

Results of the study are displayed in Tables I—II. In Table I the observed room-temperature values of ρv^2 are given for the 18 measurement modes. Table I also contains expressions for ρv^2 in terms of the C_{ij}'s. These expressions were derived from the Christoffel equations. When a plus-minus sign occurs, the plus sign corresponds to the longitudinal mode and the minus sign corresponds to the transverse mode. Estimated errors for the derived elastic constants are also in Table I. The basis for estimating these errors was described above.

Results of the resonance studies are in Table II. S_{33} is the reciprocal Young's modulus along the filament direction and $\frac{1}{2}(S_{44}+S_{55})$ is the reciprocal torsion (or shear) modulus around that direction.

The elastic compliances, S_{ij}'s, are given in Table III along with a summary of the C_{ij} data. The S_{ij}'s were determined by inverting the C_{ij} matrix displayed in Eq. (1) and substituting the C_{ij} values from Table I. Except for S_{44}, S_{55}, and S_{66}, which are simple reciprocals of the corresponding C_{ij}'s, errors in the S_{ij}'s are larger than those in the C_{ij}'s because of error accumulation.

The practical elastic constants (E = Young's modulus, G = shear modulus, and ν = Poisson's ratio) are given in Table IV. These parameters are related to the S_{ij}'s as

TABLE III. Room-temperature elastic stiffnesses C_{ij} and elastic compliances S_{ij} of a NbTi/Cu composite and copper. C_{ij} units are 10^{11} N/m^2 and S_{ij} units are 10^{-11} m^2/N. Values in parentheses are derived from $2C_{44}=C_{11}-C_{12}$ and $S_{44}=2(S_{11}-S_{12})$.

	Composite		Copper[a]	
ij	C_{ij}	S_{ij}	C_{ij}	S_{ij}
11	1.834	0.924	2.006	0.780
22	1.878	0.894		
33	1.880	0.879		
44	0.416	2.404	0.477	2.096
55	0.407	2.457		
66	0.414	2.415		
12	1.056	−0.341	(1.052)	(−0.268)
13	1.039	−0.322		
23	1.041	−0.307		

[a]Reference 7.

displayed in the matrix equation

$$S_{ij}=\begin{bmatrix} 1/E_{11} & -\nu_{21}/E_{22} & -\nu_{31}/E_{33} & 0 & 0 & 0 \\ & 1/E_{22} & -\nu_{32}/E_{33} & 0 & 0 & 0 \\ & & 1/E_{33} & 0 & 0 & 0 \\ & & & 1/G_{44} & 0 & 0 \\ & & & & 1/G_{55} & 0 \\ & & & & & 1/G_{66} \end{bmatrix}, \tag{11}$$

where the S_{ij} matrix is symmetrical about its main diagonal and the Poisson ratios are defined by

$$\nu_{ij}=-S_{ij}/S_{ii} \text{ (no sum)}. \tag{12}$$

V. DISCUSSION

A. Symmetry

On the basis of its internal and external geometry, the composite appears to be orthorhombic. If an object has three mutually perpendicular twofold axes, then it belongs to the orthorhombic symmetry system. These rotation axes are labeled x, y, and z in Figs. 1 and 2. Other possible symmetry systems can be excluded. Triclinic has no symmetry axis. Monoclinic has a single

TABLE IV. Practical elastic constants: E = Young's modulus, G = shear modulus, ν = Poisson's ratio for NbTi/Cu composite in different coordinate systems at room temperature. Units are 10^{11} N/m^2, except ν's, which are dimensionless.

Elastic constant	Orthorhombic basis	Tetragonal basis	Hexagonal basis	Isotropic basis	Copper[a] values	Static results[b] (hexagonal basis)
E_{11}	1.082	1.100	1.100	1.112	1.282	1.22
E_{22}	1.119					
E_{33}	1.138	1.138	1.138			1.19
G_{44}	0.416	0.411	0.411	0.412	0.477	0.448
G_{55}	0.407					
G_{66}	0.414	0.414	(0.398)[c]			(0.431)[c]
ν_{21}	0.381	0.381	0.381			0.415
ν_{31}	0.365	0.357	0.357			0.347
ν_{32}	0.349					

[a]Reference 7.
[b]Reference 8.
[c]Quantities in parentheses are derived from given data using $G_{66}=E_{11}/2(1+\nu_{12})$.

TABLE V. Checks for various symmetries for NbTi/Cu composite. For hexagonal and cubic cases, relationships (1), (2), and (3) also hold. For an isotropic case, all eight relationships must hold, either (4) or (8) is redundant.

Symmetry system	Relationships	Ratio of LHS/RHS for NbTi/Cu
Tetragonal	(1) $C_{22}=C_{11}$	1.024 ± 0.020
	(2) $C_{55}=C_{44}$	0.978 ± 0.014
	(3) $C_{23}=C_{13}$	1.002 ± 0.040
Hexagonal	(4) $C_{66}=\frac{1}{2}(C_{11}-C_{12})$	1.064 ± 0.020
Cubic	(5) $C_{33}=C_{11}$	1.025 ± 0.007
	(6) $C_{12}=C_{13}$	1.016 ± 0.040
	(7) $C_{66}=C_{55}$	1.017 ± 0.018
Isotropic	(8) $C_{44}=\frac{1}{2}(C_{11}-C_{12})$	1.069 ± 0.016

twofold axis. Trigonal has a single threefold axis. Clearly, these three systems are less symmetrical than the composite.

Orthorhombic symmetry includes four other symmetry systems: tetragonal, hexagonal, cubic, and isotropic. Relationships among the C_{ij}'s for these systems are given in Table V together with tests of the relationships. Clearly, from Table V, none of the higher-symmetry systems can be used to describe exactly the observed C_{ij}'s, but the deviations are small for any of these four symmetry choices. The advantage of describing an object by its highest symmetry is that there are fewer independent elastic constants: six for tetragonal, five for hexagonal, three for cubic, and two for isotropic. Thus, measurements and calculations are simplified to various degrees. In Table IV, present orthorhombic results are also expressed in higher-symmetry coordinates to facilitate comparisons with other studies. When necessary, elastic constants were simply averaged.

B. Off-diagonal elastic constants

The off-diagonal ($i \neq j$) elastic constants are more difficult to determine and almost always have higher uncertainties than the diagonal ($i=j$) elastic constants. This problem is reflected in the present study in Table I. The problem arises because the off-diagonal elastic constants are not related simply to any pure mode of mechanical deformation. This is best shown in the S_{ij} matrix displayed in Eq. (11). All the diagonal S_{ij}'s are related reciprocally to either a Young's modulus or to a shear modulus; but all the off-diagonal S_{ij}'s are related to a Young's modulus and a Poisson's ratio, which is in turn determined by two other elastic constants, as shown in Eq. (12).

In the present study, another difficulty arose in determining the off-diagonal elastic constants. As shown in Table I, different values of the off-diagonal C_{ij}'s were obtained depending on whether the observed ρv_t^2 or the observed ρv_t^2 was substituted into the appropriate C_{ij} expression given in the table. For example, in the [011] direction the quasitransverse datum gave $C_{23}=0.715$, while the quasilongitudinal datum gave $C_{23}=1.041$. The C_{12} and C_{13} cases are similar. On the basis of small imprecisions of the measurements and on the basis of the correctness of the value of the third (pure shear) mode, it seemed that the off-diagonal terms should be less uncertain than this and that one of two values was perhaps correct.

To resolve this uncertainty in the off-diagonal elastic constants, an independent experiment was done: some of the S_{ij}'s were determined by a resonance method. Dilatational and shear modes were measured on a cylindrical specimen with filaments along the cylinder axis. Results shown in Table II for the torsional mode $\frac{1}{2}(S_{44}+S_{55})$ agree exactly with the value calculated from the C_{ij}'s. (The S_{ij}'s are computed from the C_{ij}'s by inverting the C_{ij} matrix). Similarly, exact agreement is also obtained for the dilatational mode S_{33} if the C_{ij} data from quasitransverse modes rather than quasilongitudinal modes are used. Thus, it was concluded that the quasitransverse velocity data are both correct and consistent with other data. However, the quasilongitudinal wave velocities are low by about 5%. This slowing can be interpreted as a longer path length in the specimen due to interactions between the quasilongitudinal waves and internal boundaries due to the presence of filaments.

C. Comparison with copper

It is useful to compare the elastic constants of the composite with those of the matrix material, unalloyed copper,[7] to determine the effects of the filaments. Comparative data are shown in Table IV. Both the Young's moduli and the shear moduli of the composite are about 15% lower than those of copper. The compressibility,

$$K=\frac{1}{9}\sum_{i,j=1,3} S_{ij}, \tag{13}$$

of the composite is about 5% higher. The off-diagonal C_{ij}'s are identical to the value for copper, within 1%. This result may be accidental since it has no obvious physical interpretation.

D. Comparison with previous studies

The elastic constants of this composite were measured by Sun and Gray[8] using static methods, assuming hexagonal symmetry, and their results are shown in Table IV. Considering the higher inaccuracies usually associated with static methods, the agreement between the two sets of data is surprisingly good. The static Young's and shear moduli are up to 9% higher than the values reported here. The largest discrepancy is in ν_{21} and is due probably to error accumulation in the computed static value. Possibly, the differences in the two data sets are real, but this cannot be decided without knowing the uncertainties of the static values. A real difference is unlikely because, ignoring dispersion effects, dynamic elastic moduli are almost always higher than static elastic moduli, and the opposite effect is observed in this case.

E. Dispersion

No dispersion effects were observed, either in the limited 5—10-MHz region that was studied or in com-

paring the MHz pulse data with the 60-kHz resonance data. By dispersion is meant the dependence of sound velocity on frequency. Dispersive effects have been reported in many composite materials; they are usually due to either relaxation or resonance effects. Their absence here is attributed to assumed coherent interfaces between the filaments and the matrix and to the small difference in acoustic impedance between the filaments and the matrix. Absence of dispersion is also consistent with the well-defined echo patterns that were obtained.

F. Relationship to similar composites

Elastic-property data have not been reported for NbTi/Cu composites with different ratios of NbTi or with different thermal-mechanical treatments. The present data can be applied to other NbTi/Cu composites through predictive schemes that relate the elastic constants of a composite to those of its components. Using the values of the NbTi elastic constants given by Sun and Gray[8] and formulas summarized by them, it follows that the present material obeys *approximately* simple rules of mixtures. Thus, similar composites would also be expected to follow these rules approximately. The present study is a useful guide to the elastic properties of any NbTi/Cu composite, but it is a source of exact elastic data only for the particular material studied. Even when the filament matrix volume ratio is adjusted for, several other variables remain that can affect elastic properties. These include the state of mechanical deformation (the number and distribution of lattice defects), composition of the NbTi filaments, preferred orientations in either the filaments or the matrix, and degree of coherency of the filament-matrix interfaces.

G. Low-temperature elastic constants

Since this composite is intended for use as a superconductor, its low-temperature elastic properties are important. Studies down to liquid-helium temperature are underway in our laboratory and results will be reported subsequently. Preliminary results are that the composite behaves on cooling *approximately* like unalloyed copper; but the magnitudes of the elastic constant changes are slightly different and there are some anomalous effects that are both reproducible and reversible.

VI. CONCLUSIONS

The chief results and conclusions of this study are as follows:

(1) Ultrasonic (5—10 MHz) waves, both dilatational and shear, can be propagated in an NbTi/Cu composite in directions parallel, perpendicular, and oblique to the filaments.

(2) Except as noted below, usual single-crystal elasticity techniques could be used to establish the complete set of elastic constants of the composite.

(3) Longitudinal waves propagated obliquely to ⟨100⟩ directions have velocities about 5% lower than expected. Obliquely propagated shear waves travel at their expected velocities.

(4) The studied composite has orthorhombic symmetry and, therefore, nine independent elastic constants; but the deviations from isotropy are small.

(5) Compared to copper, the C_{ij}'s $(i=j)$ of the composite are lower by about 7% for C_{11}, C_{22}, and C_{33}, and by about 15% for C_{44}, C_{55}, and C_{66}; but the C_{ij}'s $(i\neq j)$ are about the same. The composite's compressibility is about 5% higher than copper's.

(6) The present dynamic results agree reasonably well with existing static measurements.

(7) Advantages of combining pulse-echo measurements and resonance measurements were found.

(8) No dispersion, change of velocity with frequency, was observed.

ACKNOWLEDGMENTS

This study was supported by the Advanced Research Projects Agency of the U.S. Department of Defense. G.A. Miranda of Los Alamos kindly contributed a photomicrograph of the studied material. W.H. Gray of Oak Ridge National Laboratory contributed a critical reading of the manuscript.

*NRC-NBS Postdoctoral Research Associate, 1975—1976.

[1]L.D. Landau and E.M. Lifshitz, *Theory of Elasticity* (Pergamon, London, 1959), p. 104.
[2]J.R. Neighbors and G.E. Schacher, J. Appl. Phys. 38, 5366—5375 (1967).
[3]M.J.P. Musgrave, *Crystal Acoustics* (Holden-Day, San Francisco, 1970), p. 117—123.
[4]A.D. McInturff and G.G. Chase, J. Appl. Phys. 44, 2378—2384 (1973).
[5]E.R. Naimon, W.F. Weston, and H.M. Ledbetter, Cryogenics 14, 246—249 (1974).
[6]J. Marx, Rev. Sci. Instrum. 22, 503—509 (1951).
[7]H.M. Ledbetter and E.R. Naimon, J. Phys. Chem. Ref. Data 3, 897—935 (1974).
[8]C.T. Sun and W.H. Gray, Sixth Symposium on Engineering Problems of Fusion Research, San Diego, Calif., 1975 (unpublished); W.H. Gray and C.T. Sun, Oak Ridge National Lab. Report TM-5331, 1976 (unpublished).